ACS APPLIED MATERIALS & INTERFACES

Letter

www.acsami.org

Improved Device Performance of Polymer Solar Cells by Using a Thin Light-harvesting-Complex Modified ZnO Film as the Cathode Interlayer

Xiaohui Liu,[†,‡] Cheng Liu,[†] Ruixue Sun,[†] Kun Liu,[†] Yajie Zhang,[‡] Hai-Qiao Wang,[‡] Junfeng Fang,[*,‡] and Chunhong Yang[*,†]

[†]Key Laboratory of Photobiology, Institute of Botany, Chinese Academy of Sciences, Beijing 100093, China

[‡]Ningbo Institute of Materials Technology and Engineering, Chinese Academy of Sciences, Ningbo 315201, China

Supporting Information

ABSTRACT: In this study, a high-performance inverted polymer solar cell (PSC) has been fabricated by incorporating a zinc oxide (ZnO)/light-harvesting complex II (LHCII) stacked structure as the cathode interlayer. The LHCII not only smoothens the film surface of ZnO, improves the contact between ZnO and the photoactive layer, but also suppresses the charge carrier recombination at the interface, hence all the device parameters of PTB7-based solar cells are simultaneously improved, yielding higher power conversion efficiency (PCE) up to 9.01% compared with the control one (PCE 8.01%). And the thin LHCII modification layer also presents similar positive effects in the PTB7-Th:$PC_{71}BM$ system (PCE from 8.31% to 9.60%). These results put forward a facile approach to the interfacial modification in high-performance PSCs and provide new insight into developing and utilizing inexpensive and environmentally friendly materials from the fields of biological photosynthesis.

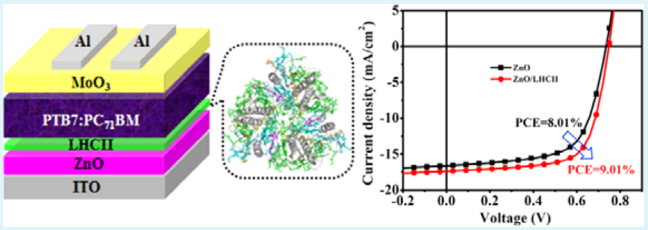

KEYWORDS: *ZnO nanoparticles, LHCII, modification interlayer, cathode, inverted polymer solar cells*

Polymer solar cells (PSCs) have received considerable attention due to their advantages of low cost, light weight, mechanical flexibility, and large-scale fabrication capability.[1−3] Although significant progresses have been achieved for this technique in the past decade, with power conversion efficiency (PCE) exceeding 9 and 10% for single-junction[4,5] and tandem[6] device, respectively, great efforts are still needed to overcome some intrinsic drawbacks of this technology, such as broadening the optical absorption of the solar cell and promoting further the PCE of this technique before its real application. As the most abundant membrane protein on the earth and because of its high efficiency in absorbing and transferring solar energy,[7] light-harvesting complex II (LHCII) possesses promising potential to fulfill the above requirement and assists in promoting the PSCs technique by acting as a light-harvesting component. Successful utilization of LHCII in P3HT:PCBM polymer solar cells was pioneered by Yao et al. in 2012.[8] Enhanced photocurrent due to the LHCII absorption and increased open circuit voltage (V_{oc}) due to the elevated built-in-potential were both demonstrated, resulting in improved PCE of 4.74 and 4.12% for normal and inverted solar cells respectively, compared to the PCE values of 3.52 and 1.74% of their control cells without LHCII complex. And more recently, LHCII was performed as a natural photosensitizer immobilized on TiO_2 nanostructured film in dye-sensitized solar cells (DSSCs), in which the electrons can be injected into the TiO_2 conduction band from LHCII, achieving efficiency up to 0.27%.[9,10] Nevertheless, quite limited research has been done about the application of LHCII in photovoltaics. And especially no specific work investigating the functionality of LHCII as thin modification layer in PSCs has been reported, although it possesses the advantages of naturally abundant and environment-friendly, besides its high absorption coefficient and energy transferring efficiency.[7]

It is known that thin modification layers (≤10 nm) such as SAMs,[11] conjugated polyelectrolytes (CPEs),[12] and polyethylenimine (PEI),[13] have often been combined with metal oxides, conducting oxides or metals in photovoltaic devices as they can modify electrode's work function,[14] saturate defect states at the interface,[15] or change the surface energy for different wetting properties,[16] hence can improve the device performance. Various materials like fullerene derivative,[17] poly(ethylene oxide) (PEO),[18] 3-aminopropanioc acid,[19] ionic liquid (ILs),[20] and cesium stearate (CsSt)[21] have been widely used to modify the ZnO layer to restrain the surface traps and improve the contact between ZnO and the active layer. We consider LHCII could possess promising potential as modification layer because of its above-mentioned properties. And moreover, a thin LHCII modification layer will contribute less to the series resistance compared to a relative thick LHCII

Received: July 3, 2015
Accepted: August 20, 2015
Published: August 20, 2015

DOI: 10.1021/acsami.5b05969
ACS Appl. Mater. Interfaces 2015, 7, 18904−18908

light harvesting layer, which otherwise decreases the device performance hugely.

In this work, we report the utilization of pure biological pigment−protein complex, LHCII, as a thin modification layer combined with wildly used ZnO interlayer in PSCs. We focus our study here on the effect of thin LHCII modification layer on the interface property and device performance of inverted structure devices, to investigate and explore the functionality and application potential of this class of material in photovoltaics.

Semiconducting polymer thieno[3,4-*b*]thiophene/benzodithiophene (PTB7) blended with [6,6]-phenyl C_{71}-butyric acid methyl ester ($PC_{71}BM$) is chosen as the active material because of its promising photovoltaic performance due to its excellent optoelectronic properties.[3] And more importantly, for this active material system the thermal annealing process is unnecessary, and thus the heat inactivation effect of LHCII can be avoid,[8] showing better compatibility with LHCII complex. Optoelectronic properties of the interlayer were characterized to study the functionality of the LHCII modification layer and relative mechanisms were discussed. High performance (enhanced by 12.5%) of our device with PCE over 9% was obtained with thin LHCII modification layer due to the increased parameters of V_{oc}, J_{sc}, and FF, compared with the control device without LHCII (PCE 8.01%), under simulated solar illumination (AM 1.5G 100 mW/cm^2). These results demonstrate the functionality of LHCII protein complex as a thin modification layer in PSCs, and suggest a promising potential for this new class of inexpensive and environment-friendly materials as modification layers in photovoltaics to improve the device performance.

The molecular structure of electron donor PTB7 and electron acceptor $PC_{71}BM$ are shown in Figure 1a. The crystal structure of LHCII assembled with specific folded protein skeleton and pigments is presented in Figure 1a as well. Figure 1b depicts the configuration of the inverted device structure adopted in our study. The thin LHCII complex layer is used to modify the ZnO interlayer and the 10 nm thick MoO_3 deposited on top of the active layer is used to facilitate the hole collection. The UV−vis-NIR absorption spectra (300−850 nm) of pure ZnO and ZnO/LHCII film on ITO substrate together with the absorption spectrum of LHCII aqueous solution are shown in Figure S1. Two main bands located at ∼370−510 nm and ∼640−690 nm are recorded for the LHCII aqueous solution. Both pure ZnO and ZnO/LHCII films show very weak absorption in the range of 400−850 nm, suggesting that most of the solar photons will pass the interlayer and contribute to the device performance. However, slightly enhanced absorption in the range of ∼370−510 nm and ∼640−690 nm can still be observed for the LHCII modified substrate compared to the pure ZnO one, which shows the presence of LHCII thin layer after the deposition.

The functionality of the LHCII modification layer in devices was confirmed by measuring the *J*−*V* curve of devices (Figure 2). To investigate the influence of LHCII film thickness on the device performance, we used different concentrations of LHCII solutions to deposit on top of the ZnO cathode interlayer by spin coating at a speed of 1000 rpm for 60 s, and the relative thickness of LHCII layer is shown in Table S1. The optimal concentration of LHCII is determined to be 0.05 mg/mL (∼6

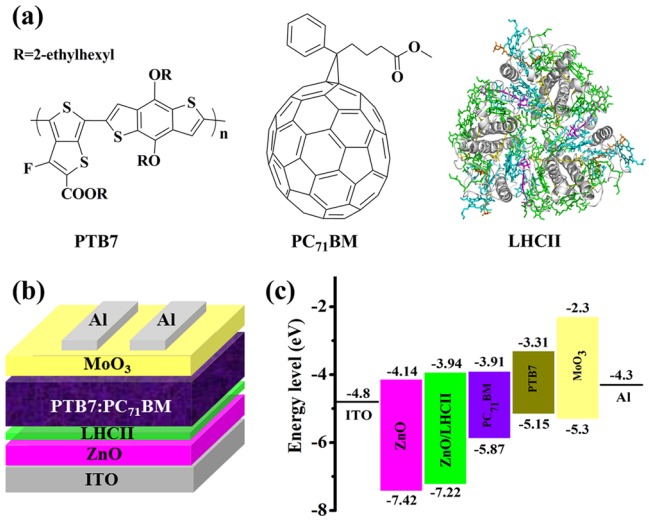

Figure 1. (a) Molecular structure of PTB7 and $PC_{71}BM$ and the crystal structure of LHCII. (b) Device structure of inverted PSCs with LHCII modified ZnO films as the stacked cathode interlayer. (c) Energy levels diagram of the components involved in the inverted device.

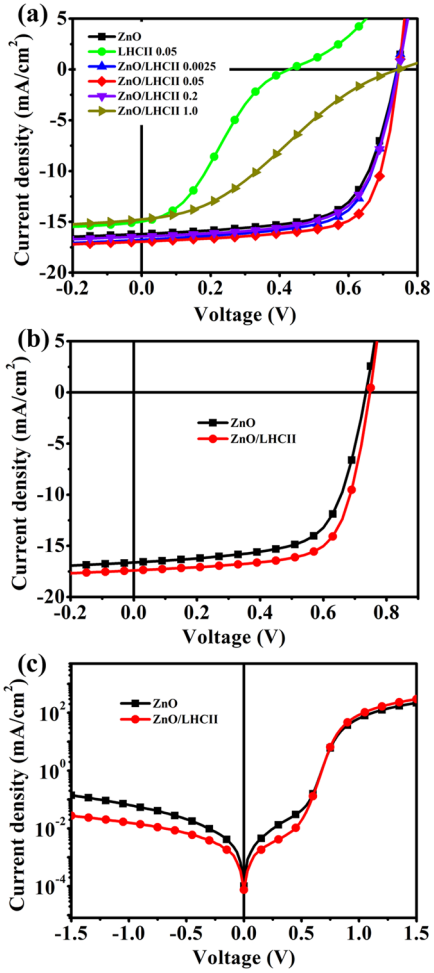

Figure 2. (a) *J*−*V* characteristics of ITO/Interlayer/PTB7:$PC_{71}BM$/MoO_3/Al architecture with different cathode interlayers (pure ZnO, pure LHCII 0.05, and ZnO/LHCII (concentration of 0.0025, 0.05, 0.2, and 1.0 mg/mL)). (b) Illuminated and (c) dark *J*−*V* characteristics of devices with different cathode interlayers (pure ZnO and optimal ZnO/LHCII).

DOI: 10.1021/acsami.5b05969
ACS Appl. Mater. Interfaces 2015, 7, 18904−18908

Table 1. Photovoltaic Parameters of PTB7:$PC_{71}BM$ Devices Fabricated with ZnO and ZnO/LHCII Interlayer Measured under 100 mW/cm^2 AM 1.5G Illumination

interlayer	V_{oc} (V)	J_{sc} (mA/cm^2)	FF (%)	PCE (%) best (average)[a]	R_s (Ω cm^2)	R_{sh} (kΩ cm^2)	RR[b] (× 10^3dark)
ZnO	0.735	16.60	65.6	8.01(7.87 ± 0.16)	5.97	0.58	1.57
ZnO/LHCII	0.748	17.39	69.3	9.01(8.91 ± 0.13)	5.28	0.68	10.79

[a]The parameters of PSCs were averaged over ten devices. [b]The rectification ratio (RR, defined as the ratio of forward-to-reverse bias current density at a bias voltage of ±1.5 V) was obtained from dark $J-V$ characteristics.

nm) and with which the ZnO/LHCII stacked film delivers the optimal device performance. With thicker LHCII modification layer or pure LHCII interlayer without ZnO, drastically decreased device performance is obtained because of the hugely decreased FF (for both devices) and V_{oc} (for pure LHCII interlayer device), which is consistent with the observed largely increased series resistance and decreased shunt resistance (Figure 2a and Table S2). With the thickest LHCII film (approximately 58 nm), the device presents a large R_s of 84.59 Ω·cm^2, resulting in an extremely low PCE of 3.34%. It should be noted that the sole LHCII interlayer cannot provide a proper diode anymore, only delivering a PCE of 1.87%, which could be attributed to the nonohmic contact between the electrode and active layer in this case.

Figure 2b presents the $J-V$ curve of the optimal device. Compared to the PCE 7.87 ± 0.16% of the control device based on pure ZnO interlayer, unambiguous enhancement in PCE (8.91 ± 0.13%) is observed after the deposition of LHCII (0.05 mg/mL) due to the promoted photovoltaic parameters of V_{oc} (from 0.735 to 0.748 V), J_{sc} (from 16.60 to 17.39 mA/cm^2) and FF (from 65.6% to 69.3%), as summarized in Table 1. More data about the distribution of different parameters of both interlayer based devices are summarized in Figure S2, each based on 10 devices. The EQE spectra of the devices based on pure ZnO and optimal ZnO/LHCII interlayer are shown in Figure S3. The ZnO/LHCII interlayer based device presents a substantial enhancement in EQE in the wavelength range of 365−705 nm compared with the pure ZnO interlayer device, corresponding to a larger photocurrent density, which is consistent with the measured J_{sc}, as shown in Figure 2b. The above results show the superior interface properties and the improved electron transfer capability of the LHCII modification interlayer, resulting in higher device efficiency. Figure 2c depicts the dark $J-V$ characteristics of ZnO and ZnO/LHCII devices. Better diode characteristics are demonstrated for the LHCII-modified ZnO-interlayer device by its lower leakage current density and higher rectification ratio (value ∼10 790), compared to the pure ZnO interlayer based device. And again the improved diode properties are confirmed by the lowered series resistance (R_s) and increased shunt resistance (R_{sh}) (Table 1).

To further understand how the LHCII modification layer affects the device performance, we carried out measurements to study the optoelectronic properties at the interface before and after the LHCII deposition. The HOMO/LUMO levels of the pure ZnO and ZnO/LHCII interlayer were determined to be −7.53/−4.14 and −7.42/−3.94 eV from the UPS (Figure S4 and Table S3) and UV−vis−NIR absorption (Figure S1) spectra, suggesting a downward vacuum level shift and a lowered work function (WF) for the LHCII modified ITO/ZnO cathode probably due to the formation of interfacial dipole. This would be beneficial for enhancing the built-in potential in device thus contributes to the V_{oc}, and which is consistent with the obtained V_{oc} (Table 1).[22] The intermediate energy gradient introduced by LHCII will facilitate the electron collection at the cathode, evidenced by the measured current density. The detailed energy level alignments of the materials in devices are summarized in Figure 1c.[3,23]

On the other hand, the surface morphology of the interlayers was studied by AFM. Figure 3a, b present the height images

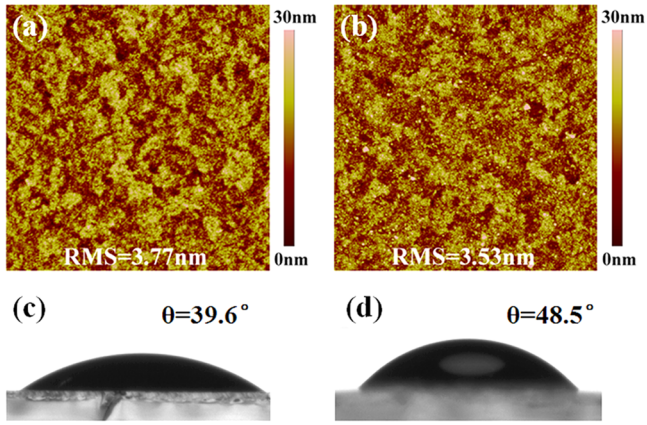

Figure 3. AFM tapping mode images (5.0 × 5.0 μm^2) of the surface morphology of (a) ZnO and (b) ZnO/LHCII surface, respectively. The RMS roughness was signed in each image (height bar of 30 nm). Contact angle images by dropping deionized water on the surface of (c) ZnO and (d) ZnO/LHCII.

(5.0 × 5.0 μm^2) of the ZnO and ZnO/LHCII interlayer on ITO substrate respectively, obtained with a tapping mode. In the case of pure ZnO film, a root-mean-square (RMS) roughness of 3.77 nm was determined. And after the deposition of LHCII, a smoother film surface was observed with a RMS roughness of 3.53 nm. The result suggested that the LHCII modification could achieve the better surface morphology of the ZnO film, which would further affect the morphology of the active layer. Besides which, a more hydrophobic film property was confirmed for the LHCII modified interlayer by its larger contact angle with water drop, compared to the pure ZnO interlayer, which could be a result of the intrinsic hydrophobic group of skeleton protein of LHCII,[7,24] as shown in Figure 3c and 3d. Consequently, this enhanced hydrophobicity would benefit the spreading of active materials on the interlayer and form better interface contact (Figure S5), thus benefit the device performance, with decreased R_s and increased FF.

To further scrutinize the underlying mechanism responsible for the enhanced performance of the devices with thin LHCII modification layer, we studied the maximum exciton generation rate (G_{max}) and exciton dissociation probability (P) in devices with pure ZnO and ZnO/LHCII as the cathode interlayer. Figure 4a demonstrates the influence of LHCII on the photocurrent density (J_{ph}) with respect to the effective voltage ($V_0 - V$), where V is the applied voltage and V_0 is the compensation voltage at which $J_L = J_D$.[25] J_{ph} is determined by

DOI: 10.1021/acsami.5b05969
ACS Appl. Mater. Interfaces 2015, 7, 18904−18908

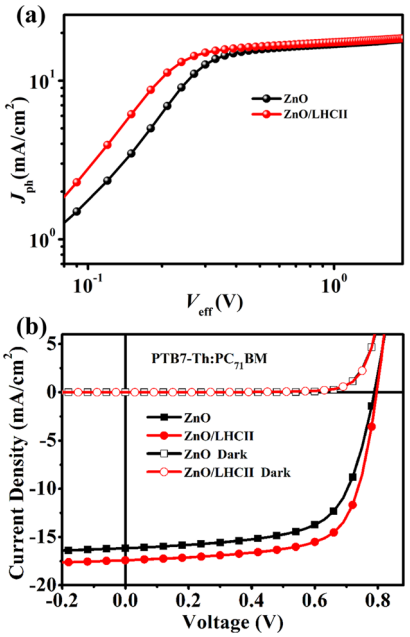

Figure 4. (a) Plots of photocurrent density (J_{ph}) with respect to the effective bias (V_{eff}) in the devices with ZnO and ZnO/LHCII as the cathode interlayer. (b) Illuminated and dark $J-V$ characteristics of ITO/Interlayer/PTB7-Th:$PC_{71}BM$/MoO_3/Al architecture with different cathode interlayers (ZnO and ZnO/LHCII).

the formula $J_{ph} = J_L - J_D$ where J_L and J_D represent the current density measured under illumination and in dark condition, respectively. Along with the increasing effective voltage, the photocurrents in two devices increased rapidly, indicating more excitons are dissociated into free carriers and better carrier collection efficiency at the interface. More details, the observed higher J_{ph} and faster reached saturation value (J_{sat}) of the ZnO/LHCII device compared to the ZnO device, suggests more effect exciton dissociation and carriers collection due to the improved interface properties by the LHCII modification. Generally, the saturated photocurrent is positively correlated to the G_{max}, which can be obtained from $J_{sat} = qG_{max}L$, where q is the electronic charge and L is the thickness of blend active layer.[25,26] It should be noted that slightly increased J_{sat} was determined for the ZnO/LHCII device in our experiment according to the double logarithmic plot (Figure 4a), which we consider could be attributed to an optical spacer effect by the introduced LHCII layer, by which the optical filed in the active layer could have been enhanced, thus increased the light absorption and G_{max}.[27,28] The values of J_{sat} and corresponding G_{max} for the devices are shown in Table S4. Simultaneously, the exciton dissociation probability (P) (i.e., V_{eff} = 1.5 V) can be got from the normalized photocurrent density J_{ph}/J_{sat}. Under the short-circuit condition, the P values are improved by LHCII passivating the traps of ZnO surface, which decrease the exciton recombination rate. Therefore, the enhanced values in G_{max} and P led to the improvement of the device performance.

Moreover, the device stability was studied for the ZnO/LHCII-based solar cells, by monitoring the device power conversion efficiency versus storage time in an argon atmosphere glovebox. Comparable and slightly improved stability was observed for the ZnO/LHCII-based device, compared to the pure ZnO-based device. And both still remain over 75% of their original PCE values after 40 days degradation (Figure S6).

And in addition, the universality of this protein complex as thin modification layer in the photovoltaics was examined with another promising active blend system of PTB7-Th:$PC_{71}BM$,[29,30] based on the same processing parameters for each layers as used in the PTB7:$PC_{71}BM$ system. Thus, the $J-V$ characteristics of the inverted PTB7-Th:$PC_{71}BM$ devices with pure ZnO and ZnO/LHCII cathode interlayer were tested in the illuminated and dark condition, respectively (Figure 4b). Again, promoted device performance can be achieved for the ZnO/LHCII-based device with a PCE of 9.60%, compared to the control device (PCE 8.31%). The key parameters are presented in Table S5. Obviously, the thin interfacial modification material of LHCII does work for different active layers system. It turns out that we could utilize the environmentally friendly biological complexes as promising material to fabricate high-performance photovoltaic devices.

In conclusion, a natural pigment−protein complex, LHCII, was successfully applied as modification layer between ZnO and photoactive layer. With the thin LHCII modification layer, simultaneous enhancement in V_{oc}, J_{sc}, and FF has been achieved for the inverted PSCs, due to the improved interfacial properties, as demonstrated by our studies in film morphology, characteristic $J-V$ parameters, and the exciton generation and dissociation properties. And this function of the thin LHCII modification layer could also be extended to the PTB7-Th:$PC_{71}BM$ system. These results indicate that the biological LHCII complexes possess a good potential to be used as electrode modifying material for high efficient PSCs. This study provides an excellent instance for exploiting and developing neotype, natural, rich-stored, and environmentally friendly materials from the biological photosynthetic fields for highly efficient PSCs.

■ ASSOCIATED CONTENT

Supporting Information

The Supporting Information is available free of charge on the ACS Publications website at DOI: 10.1021/acsami.5b05969.

Experimental details, UV−vis−NIR spectra, table of PSCs parameters with different LHCII concentration, device parameters distribution map, EQE, UPS spectra and table of energy levels, AFM images of PTB7:$PC_{71}BM$, table of summary of J_{sat}, G_{max}, P, device stability, and photovoltaic parameters of PTB7-Th:$PC_{71}BM$ devices (PDF)

■ AUTHOR INFORMATION

Corresponding Authors

*E-mail: yangch@ibcas.ac.cn.
*E-mail: fangjf@nimte.ac.cn.

Notes

The authors declare no competing financial interest.

■ ACKNOWLEDGMENTS

This research was supported by the National Basic Research Program of China (2011CBA00904), the Key Research Program of the Chinese Academy of Sciences (KSZD-EW-Z-018 and KGZD-EW-T05), and the Ningbo Agricultural Key Science and Technology Program (2013C11035). The work was also supported by Hundred Talent Program of Chinese Academy of Sciences.

DOI: 10.1021/acsami.5b05969
ACS Appl. Mater. Interfaces 2015, 7, 18904−18908

REFERENCES

(1) Gräetzel, M.; Janssen, R. A.; Mitzi, D. B.; Sargent, E. H. Materials Interface Engineering for Solution-Processed Photovoltaics. *Nature* **2012**, *488*, 304−312.

(2) Dang, M. T.; Hirsch, L.; Wantz, G.; Wuest, J. D. Controlling the Morphology and Performance of Bulk Heterojunctions in Solar Cells. Lessons Learned from the Benchmark Poly (3-Hexylthiophene):[6, 6]-Phenyl-C_{61}-Butyric Acid Methyl Ester System. *Chem. Rev.* **2013**, *113*, 3734−3765.

(3) Liang, Y.; Xu, Z.; Xia, J.; Tsai, S. T.; Wu, Y.; Li, G.; Ray, C.; Yu, L. For the Bright Future-Bulk Heterojunction Polymer Solar Cells with Power Conversion Efficiency of 7.4%. *Adv. Mater.* **2010**, *22*, E135−E138.

(4) He, Z.; Zhong, C.; Su, S.; Xu, M.; Wu, H.; Cao, Y. Enhanced Power-Conversion Efficiency in Polymer Solar Cells using an Inverted Device Structure. *Nat. Photonics* **2012**, *6*, 591−595.

(5) Ye, L.; Zhang, S.; Zhao, W.; Yao, H.; Hou, J. Highly Efficient 2D-Conjugated Benzodithiophene-Based Photovoltaic Polymer with Linear Alkylthio Side Chain. *Chem. Mater.* **2014**, *26*, 3603−3605.

(6) You, J.; Dou, L.; Yoshimura, K.; Kato, T.; Ohya, K.; Moriarty, T.; Emery, K.; Chen, C.-C.; Gao, J.; Li, G. A Polymer Tandem Solar Cell with 10.6% Power Conversion Efficiency. *Nat. Commun.* **2013**, *4*, 1446−1455.

(7) Liu, Z.; Yan, H.; Wang, K.; Kuang, T.; Zhang, J.; Gui, L.; An, X.; Chang, W. Crystal Structure of Spinach Major Light-Harvesting Complex at 2.72 Å Resolution. *Nature* **2004**, *428*, 287−292.

(8) Yao, K.; Liu, C.; Chen, Y.; Chen, L.; Li, F.; Liu, K.; Sun, R.; Wang, P.; Yang, C. Integration of Light-Harvesting Complexes into the Polymer Bulk Heterojunction P3HT/PCBM Device for Efficient Photovoltaic Cells. *J. Mater. Chem.* **2012**, *22*, 7342−7349.

(9) Nagata, M.; Amano, M.; Joke, T.; Fujii, K.; Okuda, A.; Kondo, M.; Ishigure, S.; Dewa, T.; Iida, K.; Secundo, F.; Amao, Y.; Hashimoto, H.; Nango, M. Immobilization and Photocurrent Activity of a Light-Harvesting Antenna Complex II, LHCII, Isolated from a Plant on Electrodes. *ACS Macro Lett.* **2012**, *1*, 296−299.

(10) Yu, D.; Zhu, G.; Liu, S.; Ge, B.; Huang, F. Photocurrent Activity of Light-Harvesting Complex II Isolated from Spinach and Its Pigments in Dye-Sensitized TiO_2 Solar Cell. *Int. J. Hydrogen Energy* **2013**, *38*, 16740−16748.

(11) Stubhan, T.; Salinas, M.; Ebel, A.; Krebs, F. C.; Hirsch, A.; Halik, M.; Brabec, C. J. Increasing the Fill Factor of Inverted P3HT: PCBM Solar Cells Through Surface Modification of Al-Doped ZnO via Phosphonic Acid-Anchored C60 SAMs. *Adv. Energy Mater.* **2012**, *2*, 532−535.

(12) Choi, H.; Park, J. S.; Jeong, E.; Kim, G.-H.; Lee, B. R.; Kim, S. O.; Song, M. H.; Woo, H. Y.; Kim, J. Y. Combination of Titanium Oxide and a Conjugated Polyelectrolyte for High-Performance Inverted-Type Organic Optoelectronic Devices. *Adv. Mater.* **2011**, *23*, 2759−2763.

(13) Zhou, Y.; Fuentes-Hernandez, C.; Shim, J.; Meyer, J.; Giordano, A. J.; Li, H.; Winget, P.; Papadopoulos, T.; Cheun, H.; Kim, J.; Fenoll, M.; Dindar, A.; Haske, W.; Najafabadi, E.; Khan, T. M.; Sojoudi, H.; Barlow, S.; Graham, S.; Brédas, J.-L.; Marder, S. R.; Kahn, A.; Kippelen, B. A Universal Method to Produce Low-Work Function Electrodes for Organic Electronics. *Science* **2012**, *336*, 327−332.

(14) Huang, J.; Li, G.; Yang, Y. A Semi-Transparent Plastic Solar Cell Fabricated by a Lamination Process. *Adv. Mater.* **2008**, *20*, 415−419.

(15) Lu, L. P.; Kabra, D.; Friend, R. H. Barium Hydroxide as an Interlayer Between Zinc Oxide and a Luminescent Conjugated Polymer for Light-Emitting Diodes. *Adv. Funct. Mater.* **2012**, *22*, 4165−4171.

(16) Savva, A.; Petraki, F.; Elefteriou, P.; Sygellou, L.; Voigt, M.; Giannouli, M.; Kennou, S.; Nelson, J.; Bradley, D. D.; Brabec, C. J. The Effect of Organic and Metal Oxide Interfacial Layers on the Performance of Inverted Organic Photovoltaics. *Adv. Energy Mater.* **2013**, *3*, 391−398.

(17) Hau, S. K.; Cheng, Y.-J.; Yip, H.-L.; Zhang, Y.; Ma, H.; Jen, A. K. Y. Effect of Chemical Modification of Fullerene-Based Self-Assembled Monolayers on the Performance of Inverted Polymer Solar Cells. *ACS Appl. Mater. Interfaces* **2010**, *2*, 1892−1902.

(18) Shao, S.; Zheng, K.; Pullerits, T.; Zhang, F. Enhanced Performance of Inverted Polymer Solar Cells by Using Poly(ethylene oxide)-Modified ZnO as an Electron Transport layer. *ACS Appl. Mater. Interfaces* **2013**, *5*, 380−385.

(19) Zuo, L.; Gu, Z.; Ye, T.; Fu, W.; Wu, G.; Li, H.; Chen, H. Enhanced Photovoltaic Performance of $CH_3NH_3PbI_3$ Perovskite Solar Cells through Interfacial Engineering using Self-Assembling Monolayer. *J. Am. Chem. Soc.* **2015**, *137*, 2674−2679.

(20) Yu, W.; Huang, L.; Yang, D.; Fu, P.; Zhou, L.; Zhang, J.; Li, C. Efficiency Exceeding 10% for Inverted Polymer Solar Cells with a ZnO/Ionic Liquid Combined Cathode Interfacial Layer. *J. Mater. Chem. A* **2015**, *3*, 10660−10665.

(21) Wang, G.; Jiu, T.; Tang, G.; Li, J.; Li, P.; Song, X.; Lu, F.; Fang, J. Interface Modification of ZnO-Based Inverted PTB7:$PC_{71}BM$ Organic Solar Cells by Cesium Stearate and Simultaneous Enhancement of Device Parameters. *ACS Sustainable Chem. Eng.* **2014**, *2*, 1331−1337.

(22) O'Malley, K. M.; Li, C. Z.; Yip, H. L.; Jen, A. K. Y. Enhanced Open-Circuit Voltage in High Performance Polymer/Fullerene Bulk-Heterojunction Solar Cells by Cathode Modification with a C_{60} Surfactant. *Adv. Energy Mater.* **2012**, *2*, 82−86.

(23) Tao, C.; Ruan, S.; Zhang, X.; Xie, G.; Shen, L.; Kong, X.; Dong, W.; Liu, C.; Chen, W. Performance Improvement of Inverted Polymer Solar Cells with Different Top Electrodes by Introducing a MoO_3 Buffer Layer. *Appl. Phys. Lett.* **2008**, *93*, 193307.

(24) Gordiichuk, P. I.; Wetzelaer, G.-J. A. H.; Rimmerman, D.; Gruszka, A.; de Vries, J. W.; Saller, M.; Gautier, D. A.; Catarci, S.; Pesce, D.; Richter, S.; Blom, P. W. M.; Herrmann, A. Solid-State Biophotovoltaic Cells Containing Photosystem I. *Adv. Mater.* **2014**, *26*, 4863−4869.

(25) Xu, M. F.; Zhu, X. Z.; Shi, X. B.; Liang, J.; Jin, Y.; Wang, Z. K.; Liao, L. S. Plasmon Resonance Enhanced Optical Absorption in Inverted Polymer/Fullerene Solar Cells with Metal Nanoparticle-Doped Solution-Processable TiO_2 Layer. *ACS Appl. Mater. Interfaces* **2013**, *5*, 2935−2942.

(26) He, Z.; Zhong, C.; Huang, X.; Wong, W. Y.; Wu, H.; Chen, L.; Su, S.; Cao, Y. Simultaneous Enhancement of Open-Circuit Voltage, Short-Circuit Current Density, and Fill Factor in Polymer Solar Cells. *Adv. Mater.* **2011**, *23*, 4636−4643.

(27) Kim, J. Y.; Kim, S. H.; Lee, H.-H.; Lee, K.; Ma, W.; Gong, X.; Heeger, A. J. New Architecture for High-Efficiency Polymer Photovoltaic Cells Using Solution-Based Titanium Oxide as an Optical Spacer. *Adv. Mater.* **2006**, *18*, 572−576.

(28) Chuang, M.-K.; Chen, F.-C. Synergistic Plasmonic Effects of Metal Nanoparticle-Decorated PEGylated Graphene Oxides in Polymer Solar Cells. *ACS Appl. Mater. Interfaces* **2015**, *7*, 7397−7405.

(29) He, Z.; Xiao, B.; Liu, F.; Wu, H.; Yang, Y.; Xiao, S.; Wang, C.; Russell, T. P.; Cao, Y. Single-Junction Polymer Solar Cells with High Efficiency and Photovoltage. *Nat. Photonics* **2015**, *9*, 174−179.

(30) Chen, J. D.; Cui, C.; Li, Y. Q.; Zhou, L.; Ou, Q. D.; Li, C.; Li, Y.; Tang, J. X. Single-Junction Polymer Solar Cells Exceeding 10% Power Conversion Efficiency. *Adv. Mater.* **2015**, *27*, 1035−1041.

DOI: 10.1021/acsami.5b05969
ACS Appl. Mater. Interfaces 2015, 7, 18904−18908